

Conformational disorder of conjugated polymers: Implications for optical properties

Sophia N. Yaliraki and Robert J. Silbey

Citation: *J. Chem. Phys.* **104**, 1245 (1996); doi: 10.1063/1.470782

View online: <http://dx.doi.org/10.1063/1.470782>

View Table of Contents: <http://jcp.aip.org/resource/1/JCPSA6/v104/i4>

Published by the [American Institute of Physics](#).

Additional information on *J. Chem. Phys.*

Journal Homepage: <http://jcp.aip.org/>

Journal Information: http://jcp.aip.org/about/about_the_journal

Top downloads: http://jcp.aip.org/features/most_downloaded

Information for Authors: <http://jcp.aip.org/authors>

ADVERTISEMENT



**ACCELERATE COMPUTATIONAL CHEMISTRY BY 5X.
TRY IT ON A FREE, REMOTELY-HOSTED CLUSTER.**

[LEARN MORE](#)

Conformational disorder of conjugated polymers: Implications for optical properties

Sophia N. Yaliraki and Robert J. Silbey

Department of Chemistry and Center for Materials Science and Engineering, Massachusetts Institute of Technology, Cambridge, Massachusetts 02139

(Received 21 August 1995; accepted 20 October 1995)

A physical picture of a conjugated chain as a collection of almost planar segments, separated by large angular breaks arises from a microscopic model which includes conjugation and steric interactions. The conjugation part of the standard phenomenological Hamiltonian for torsional motion is also derived from the model. We obtain a probability distribution of the length of segments between those breaks as the relevant factor for the behavior of the chain. We also perform numerical simulations of the structure and properties of these chains; the results of this are in agreement with our analytic predictions. In explaining experimental data for optical properties, such as the second hyperpolarizability, γ , our theory provides improved agreement over previous models. © 1996 American Institute of Physics. [S0021-9606(96)51804-5]

I. INTRODUCTION

The effects of conformational disorder on the electronic properties of conjugated polymers has been the focus of various studies.¹⁻⁵ In some cases, the extent of the effect has been shown theoretically to be small,⁶ and, since deviations from planar configurations on these systems are small, they have therefore been ignored. Since small deviations from planarity have little effect on the conjugation, and large deviations have a great effect, then for the study of nonlinear optical properties, the large deviations, although rare, are determinative. This leads to a model for the optical properties of the conjugated chain that can be described as relatively long, almost planar segments (perhaps “wormlike”) separated by abrupt breaks in planarity (“flips”). It is the flips that dominate the optical properties. This is different in spirit to the work of Soos and Schweizer,⁷ who consider the chain as “wormlike” without large rotational defects that break the conjugation. This alternative description challenges the idea of one effective length as adequate characterization of the properties of conjugated systems. Our work also differs to that of Kohler *et al.*,⁸ where distributions of conjugation length were varied to best fit measured absorption spectra. Here, we derive a probability distribution of segments beginning from a microscopic Hamiltonian, that we believe contains the most relevant interactions of our problem. This picture leads to an improved explanation of optical properties of long chains as seen in recent experiments.⁹

We consider systems with alternating single and double bonds. Rotation around each single bond is allowed; a plane or platelet is associated with each double bond. Although we choose polyacetylene to illustrate the model, we are not confined to this system. Any monomeric unit, such as a ring, can be the building block of the platelet. Each platelet forms an angle θ with the reference plane of the perfectly planar chain; adjacent platelets form a relative angle ϕ (Fig. 1). A tight binding model with modified transfer integrals (to accommodate rotations) is used to describe the electronic behavior of the system. A torsional potential takes into account steric

effects arising from the rotation of platelets. Electron correlations are ignored at this level. We show that the “fragmented” chain constitutes a meaningful picture for these systems, and apply it to the calculation of optical properties such as the absorption spectrum, the linear polarizability, α , and the second hyperpolarizability, γ . We also study the effect of conformational disorder for this system through numerical simulations, using a Metropolis-type algorithm. We compare our analytical results to those from the simulations as well as to experiments and show good agreement.

The paper is structured as follows: in Sec. II we present the microscopic model Hamiltonian of conjugation and steric interactions. We derive from this Hamiltonian the phenomenological term used by Rossi *et al.*² to model torsional motion. In Secs. III and IV, we discuss the picture of the fragmented chain. In Sec. III we calculate the number of flips in the chain from the phenomenological model, as well as the probability distribution of the length of the conjugated segments between flips. In Sec. IV we discuss our numerical simulations performed with the original microscopic Hamiltonian and compare with the analytical results. Finally in Sec. V we calculate optical properties based on the results of our model in Sec. III and compare with experiments.

II. THE MODEL

We study the conformational behavior of a conjugated chain with allowed rotations around the single bonds, taking into account both the electronic transfer terms and steric repulsion interactions in the system as the most relevant to our purpose. It is widely accepted that, due to steric interactions, delocalization of electrons is hindered, although the manner and extent of this is yet to be fully understood. As noted above, we propose that a long chain does not distort in a continuous wormlike manner, but rather, in a disjointed fashion, forming numerous smaller than original length, almost planar segments (also referred to as “strings”), separated by sudden, local breaks (or “flips”) caused by large relative angles. Specifically, a number of consecutive platelets are

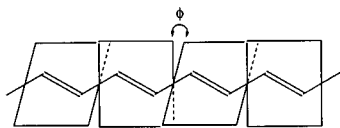


FIG. 1. Model system, adjacent platelets form a relative angle ϕ .

coplanar (to within a small angle) with those adjacent until the next one lies in a plane forming an angle of much greater magnitude than the previous ones. Then the adjacent platelets form another almost planar string until a further flip occurs, producing a distribution of angles between platelets mainly concentrated around zero, occurring in clusters, with a few outside of that range. Thus the long chain can be considered to be a collection of quasiplanar segments separated by large angle flips. The optical properties are dominated by the distribution of segment lengths; thus the precise distribution of angles within a segment is unimportant. To substantiate the proposed picture, we calculate the probability distribution of such breaks or “flips,” as well as the number and length of planar segments or “strings” in a chain of total $2N$ carbon atoms, and we compare the results with numerical experiments on the same systems. Within this picture, we are able to account for aspects of the experimental behavior of the third order polarizability γ of such conjugated systems.⁹ The implication of such an approach suggests that the idea of a single effective length for a given chain is inadequate. The chain behaves in effect, not as one of smaller than original length, but as a collection of smaller ones. In this study we neglect interactions between those segments. Also, the length of these segments may not be constant, but may change together with the configuration of the chain with time evolution. However, the ensemble of chains has a stationary probability distribution. Our simulations, discussed in Sec. IV are in good quantitative agreement with this model. Note the similarity of this picture to that of Schweizer who studied linear optical properties and phase transitions in polymers.¹⁰

We now introduce the microscopic Hamiltonian of our system. A chain of $2N$ atoms with one unpaired electron per atom is considered. The chain is treated as a one dimensional system with $2N$ sites, each occupied by an atom. The most relevant interactions for our problem are the steric interactions between adjacent groups, which tend to keep adjacent platelets away from planarity, and the delocalization of electrons, which favors the planar conformation. The electron–phonon coupling interaction is explicitly neglected, although bond dimerization is imposed. Electron–electron interactions are not considered at this stage; however we expect that they reduce delocalization, thus making the steric effect even more important and our picture more relevant.

The Hamiltonian

$$H = - \sum_{\sigma} \sum_{n=1}^N [t_d c_{n\sigma,1}^{\dagger} c_{n\sigma,2} + t_s \cos(\theta_n - \theta_{n+1}) \times c_{n\sigma,2}^{\dagger} c_{n+1\sigma,1} + \text{h.c.}] - \sum_{n=1}^N V_0 \cos(\theta_n - \theta_{n+1}) \quad (1)$$

describes the conjugation and the steric effect. Each of the N unit cells contains two carbon atoms—a double and a single bond of fixed length. The standard fermionic operators $c_{n\sigma,a}^{\dagger}$ ($c_{n\sigma,a}$) create (annihilate) an electron of spin σ on position a of unit cell n . t_s and t_d are the electron transfer integrals for single and double bonds, respectively. They can be obtained from experimental observation of the band gap through an electron–phonon coupling model like that of Su–Schrieffer–Heeger.¹¹ Notice that transfer across a single bond depends on the relative orientation of the neighboring platelets. V_0 represents an effective steric hindrance energy parameter. If the interaction is favorable, as for example in hydrogen bonding cases, $V_0 > 0$; if the steric interactions are repulsive, then either $V_0 < 0$ or we can consider a term of the form $\cos(\pi - \Delta\theta) = -\cos(\Delta\theta)$.

Our model stresses the competition between conjugation and steric interactions. We should emphasize though that, in contrast to Rossi *et al.*,² we begin from a microscopic description instead of using a phenomenological model. Rossi *et al.* study the role of conformational disorder of such systems with the use of effective potentials,

$$H_R = \sum_{n=1}^N -E_c \cos 2(\theta_n - \theta_{n+1}) - E_s \cos(\theta_n - \theta_{n+1}) \\ = H_{\text{conj}} + H_{\text{ster}}. \quad (2)$$

The form of the conjugation term agrees with our intuitive understanding; it exhibits a minimum when the platelets are aligned, and a maximum when they are perpendicular to each other. By a simple change of variables $\phi_n = \theta_n - \theta_{n+1}$, with Jacobian equal to unity, we can transform both Hamiltonians to relative angle of platelets variables, $\{\phi_i\}$.

We now derive the phenomenological Hamiltonian [Eq. (2)] from the microscopic Hamiltonian [Eq. (1)]. Starting from the electronic part of our model [Eq. (1)], through a perturbation expansion for small angles, we derive the angular dependence for the conjugation energy. Since the first term of Eq. (2) represents the change in conjugation energy caused by a conformational change, this provides justification for the use of such widely used phenomenological potentials and relates it analytically to the ratio of transfer integrals. We also show numerically, for all angles, agreement with the E_c value and with the $\cos(2\phi)$ functional dependence.

We assume that all the platelets are aligned with each other except for the two in position n_p and n_{p+1} , i.e., all ϕ_n are set to zero except for those two such that they form an angle $\phi_{n_p} = \theta_{n_p} - \theta_{n_{p+1}}$. Note that if the minimum energy angle is not $\phi=0$, but ϕ_{eq} , we can expand around ϕ_{eq} instead of $\phi=0$. The subsequent argument is unaffected. Assuming

the angles are small enough to allow for an expansion of the cos ϕ , the first term of the Hamiltonian can be expressed in the following manner:

$$H = H_0 + V(\phi),$$

$$H = - \sum_{\sigma} \sum_{n=1}^N (t_d c_{n\sigma,1}^{\dagger} c_{n\sigma,2} + t_s c_{n\sigma,2}^{\dagger} c_{n+1\sigma,1} + \text{h.c.})$$

$$+ \sum_{\sigma} \frac{t_s}{2} \phi_{n_p}^2 c_{n_p\sigma,2}^{\dagger} c_{n_p+1\sigma,1} + \text{h.c.},$$

where H_0 is the standard tight binding Hamiltonian with known exact analytic solutions for periodic boundary conditions. $V(\phi)$ can be viewed as the perturbative effect of conformational disorder on conjugation and is thus related to the phenomenological term of H_R . After making the approximation for small angles and requiring it to hold for all angles ϕ ,

$$\langle G_0 | V | G_0 \rangle = \langle G_0 | \sum_{\sigma} \frac{t_s}{2} \phi_{n_p}^2 c_{n_p\sigma,2}^{\dagger} c_{n_p+1\sigma,1} + \text{h.c.} | G_0 \rangle$$

$$= 2E_c \phi^2 \cong E_c (1 - \cos 2\phi),$$

where $|G_0\rangle$ is the ground state eigenfunction of the standard Hamiltonian H_0 . Exploiting the periodic boundary conditions, H_0 can be diagonalized with the following operators keeping in mind that there are two carbon atoms per unit cell,

$$c_{k\sigma,a} = \frac{1}{\sqrt{N}} \sum_n e^{-ikn} c_{n\sigma,a},$$

$$k = 2\pi j/N, \quad j = 0, 1, \dots, (N-1),$$

and $a = 1, 2$ stands for the position of a carbon atom in the unit cell. H_0 now becomes

$$H_0 = - \sum_{k,\sigma} (c_{k\sigma,1}^{\dagger}, c_{k\sigma,2}^{\dagger}) \begin{pmatrix} 0 & t_d + t_s e^{-ik} \\ t_d + t_s e^{ik} & 0 \end{pmatrix}$$

$$\times \begin{pmatrix} c_{k\sigma,1} \\ c_{k\sigma,2} \end{pmatrix}$$

and can be brought to diagonal form with the standard transformation

$$T = \begin{pmatrix} e^{i\alpha_k} \cos \theta_{k\sigma} & -e^{i\alpha_k} \sin \theta_{k\sigma} \\ \sin \theta_{k\sigma} & \cos \theta_{k\sigma} \end{pmatrix}$$

with

$$\tan \alpha_k = - \frac{t_s \sin k}{t_d + t_s \cos k} \quad (3)$$

and $\theta_{k\sigma} = \pi/4$. The Hamiltonian H_0 can be expressed in terms of new operators

$$H_0 = - \sum_{\sigma} \sum_{i=1,2} \sum_k E_{k\sigma,i} b_{k\sigma,i}^{\dagger} b_{k\sigma,i}$$

with

$$E_{k\sigma,j} = (-1)^j (t_d^2 + t_s^2 + 2t_s t_d \cos k)^{1/2}$$

and

$$\begin{pmatrix} b_{k\sigma,1} \\ b_{k\sigma,2} \end{pmatrix} = T^{-1} \begin{pmatrix} c_{k\sigma,1} \\ c_{k\sigma,2} \end{pmatrix}.$$

The ground state $|G_0\rangle = \prod_{k=0,\sigma}^{\leq \pi} b_{k\sigma,1}^{\dagger} |0\rangle$, where $|0\rangle$ is the vacuum state, and $b_{k\sigma,1}^{\dagger} = (1/\sqrt{2})(c_{k\sigma,1}^{\dagger} e^{i\alpha_k} + c_{k\sigma,2}^{\dagger})$. By expressing V in terms of the new operators b_{ka} , we obtain the energy correction

$$E_c = \frac{t_s}{N} \sum_k \cos(\alpha_k + k).$$

From Eq. (3),

$$\cos \alpha_k = \frac{\frac{t_d}{t_s} + \cos k}{\left[1 + \frac{t_d^2}{t_s^2} + 2\frac{t_d}{t_s} \cos k\right]^{1/2}},$$

$$\sin \alpha_k = \frac{-\sin k}{\left[1 + \frac{t_d^2}{t_s^2} + 2\frac{t_d}{t_s} \cos k\right]^{1/2}}.$$

Using the trigonometric identity for sums of cosines,

$$E_c = - \frac{1}{2N} \sum_k t_s \frac{\frac{t_d}{t_s} + \cos k}{\left[1 + \left(\frac{t_d}{t_s}\right)^2 + 2\frac{t_d}{t_s} \cos k\right]^{1/2}}.$$

Approximating the sums with integrals, we obtain

$$E_c = \frac{t_s}{4\pi} \left[\frac{1}{\frac{t_d}{t_s} + 1} K(r) + \frac{t_d}{t_s} \left(1 + \frac{t_d}{t_s}\right)^2 E(r) - \left(1 + \frac{t_d}{t_s}\right)^2 K(r) \right],$$

where $E(r)$ and $K(r)$ are the complete elliptic integrals of the first kind and second kind, respectively, with argument

$$r = \frac{2 \left[\frac{t_d}{t_s} \right]^{1/2}}{1 + \frac{t_d}{t_s}}.$$

As the physically relevant range occurs when the ratio r approaches one, we consider this limiting behavior of the elliptic integrals. For r close to one, $K(r)$ approaches $\frac{1}{2} \ln(16/1-r)$, and $E(r) \approx \frac{1}{2} \ln(16/1-r) - 1$. After some algebra, we find

$$K(r) = \ln 4 + \ln \left(\frac{\frac{t_d}{t_s} + 1}{\frac{t_d}{t_s} - 1} \right) = \ln 4 + 2 \coth^{-1} \left(\frac{t_d}{t_s} \right).$$

Similarly, $E(r) = \ln 4 + 2 \tanh^{-1}(t_d/t_s) - 1$. Finally, we set $t \equiv (t_d/t_s)$, and we obtain

$$E_c = \frac{t_s}{4\pi} \left\{ \frac{\ln 4 + 2 \coth^{-1}(t)}{1+t} + 2t^2 [\ln 4 + 2 \coth^{-1}(t)] - t(1+t)^2 \right\}. \quad (4)$$

We notice immediately the dependence of the conjugation energy per units of t_d on the ratio, t , of the transfer integrals. According to standard mean field theories (see, for example, Ref. 11) this ratio depends only on the band gap E_g and bandwidth W_g of the system

$$t_d/t_s = \frac{1 + E_g/W_g}{1 - E_g/W_g}.$$

We are thus able to connect our microscopic model to a phenomenological one whose parameters can be obtained from experimental data. By using the "standard" values for $E_g = 1.4$ eV and $W_g = 10$ eV (and $t_s = 2.15$ eV, $t_d = 2.85$ eV) for polyenes, we obtain for $E_c/N = 0.015$ eV. To check the validity of our approximations, we numerically performed the same calculation with the original Hamiltonian, and obtained the same value for E_c .

Having made the above connections, we can use the H_R Hamiltonian of Eq. (2) to study the chain under conformational disorder. Estimates for the effective steric potential parameter in solution are based on NMR spectroscopy and in the gas phase on Raman spectroscopy, as well as *ab initio* or semiempirical calculations. For example, for polyacetylene Rossi *et al.* used the value $E_s = 1.5$ kcal/mol.¹³ Here, we do not consider any particular system and we take $V_0 = 0.026$ eV, a room-temperature value. This value should be appropriately changed for each polymer.

III. FRAGMENTARY VS WORMLIKE CHAIN

A. Calculation of number of flips in a chain

To distinguish between a wormlike and a fragmentary chain, we would like to know how many abrupt changes occur in equilibrium conformations of the system. The definition of an abrupt change may seem rather arbitrary, but our results turn out to be insensitive to its absolute measure within broad limits. Crudely, one can think of bonds as completely conjugated ($\theta_i - \theta_{i+1} = 0$) or completely broken ($\theta_i - \theta_{i+1} = \pi/2$). We consider a more realistic situation; a "flip" occurs when $|\theta_i - \theta_{i+1}| > \phi_0$. In the simulations on polyacetylene, discussed in detail in Sec. IV, ϕ_0 is taken to be 10° , 15° , and 20° without qualitative difference in the results. We thus proceed to calculate the probability distribution as well as the most probable number of flips in a chain of N double bonds, using the H_R Hamiltonian [Eq. (2)].

Our model only includes nearest neighbor interactions—the relative angles of platelets are thus independent variables. The probability distribution of any angle ϕ_i is

$$P(\phi) = \frac{e^{\beta(E_c \cos 2\phi + E_s \cos \phi)}}{Z},$$

where $\beta = (1/kT)$ and $Z = \int_{-\pi}^{\pi} d\phi e^{E_c \cos 2\phi + E_s \cos \phi}$. For systems which favor a planar conformation, we expect the

angles to be small, so we expand the Hamiltonian around the minimum $\phi = 0$ (if $\phi_{eq} \neq 0$, an expansion is made around ϕ_{eq}),

$$H_R = \sum_{i=1}^N -E_c(1 - 2\phi_i^2) - E_s(1 - \phi_i^2/2).$$

The angle dependency is usually ignored because its effect on electronic properties is negligible. We will show however that, no matter how small, these angular deviations give rise to a new physical picture. A similar approach can be taken for chains with a minimum configuration other than the perfectly planar one and the qualitative behavior is the same. The probability distribution now becomes

$$P(\phi) = \frac{e^{-\beta\phi^2(E_s + 4E_c)/2}}{\int_{-\pi}^{\pi} d\phi e^{-\beta\phi^2(E_s + 4E_c)/2}}. \quad (5)$$

We can now obtain from Eq. (5) the probability of two adjacent platelets being coplanar, and we find it to be $P(0) = 0.72$. From the numerical simulations (Sec. IV), we also observe approximately 70% of the angles to be around zero. Such clustering of the relative angles of platelets around zero reinforces the fragmented chain picture.

We now calculate the most probable number of flips or breaks, m^* , in conjugation in the chain. Consider an open chain, so there are $N-1$ single bonds. If all platelets were coplanar, the energy of the system would be

$$E = -(N-1)(E_s + E_c).$$

If one flip occurs, then $E = -(N-2)(E_s + E_c) - E_s \cos \phi - E_c \cos 2\phi$. For m flips,

$$E = -(N-m-1)(E_s + E_c) - \sum_{i=1}^m (E_s \cos \phi_i + E_c \cos 2\phi_i).$$

So

$$Z = \sum_m e^{(N-m-1)(E_s + E_c)/kT} e^{\beta \sum_{i=1}^m (E_s \cos \phi_i + E_c \cos 2\phi_i)} C_m^N \\ = \sum_m T_m,$$

where $C_m^{N-1} = [(N-1)!/m!(N-m-1)!]$ takes into account the different ways m flips can occur in $N-1$ possible sites. In Fig. 2, we notice that this distribution of flips agrees very well with that obtained from the results of numerical experiments described in detail in Sec. IV. After making Stirling's approximation, we obtain for the most probable number of flips, m^* ,

$$\frac{dT_m}{dm} = 0 \Rightarrow \frac{m^*}{N} \approx e^{-(E_s + E_c)/kT}. \quad (6)$$

Since E_s is directly related to V_0 and E_c to (t_d/t_s) according to relation (4), our result is immediately connected to our original model. Note that as the temperature T increases, more flips are expected to occur. Similarly, a longer chain can support more flips. These results agree with intuitive ideas of increasing disorder with increasing temperature, as well as higher number of conformational distortions at

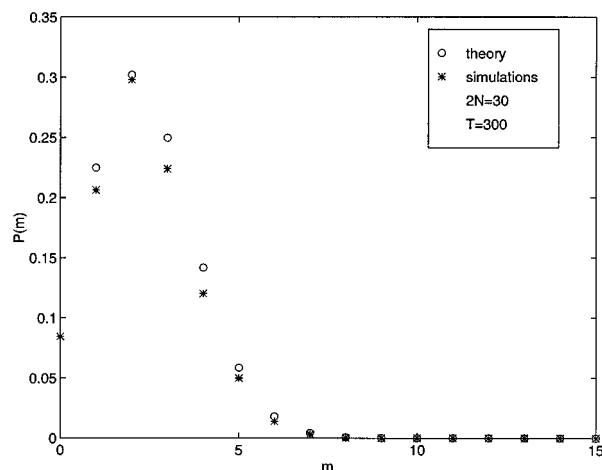


FIG. 2. Probability distribution of “flips” in a chain of 30 carbon atoms at $T=300$ K from theory and simulations

longer lengths. Additionally, we can see from the above formula that as N increases, one expects to find more planar segments (strings), instead of longer ones. So the probability distribution of lengths of the strings will eventually be independent of N . We compare the values of the most probable number of flips for a chain of 30 atoms at different temperatures between predictions of the model and numerical experiments (see Sec. IV), and find relatively good agreement. Since the long chain limit has been invoked, we expect an even better agreement for longer chains. As can be seen in Table I, the number of flips is substantial, supporting the idea of a fragmented chain.

B. Calculation of $\varphi^N(l)$

We are also interested in the probability of finding a fully conjugated segment of length l between flips in the chain. We consider such strings to be fully conjugated when the angular difference of adjacent platelets is small, i.e.,

$$|\phi_i| \leq \phi_0$$

for all i within the segment. Determining this probability distribution, $\varphi^N(l)$, is important because it will enable the calculation of experimental physical properties of these systems, such as the absorption spectrum, the linear polarizability, α , and the second hyperpolarizability, γ , described in Sec. V.

TABLE I. Most probable number of flips in a chain of 30 carbon atoms from theory and simulation.

T (K)	m_{calc}^*	m_{sim}^*
300	3	2
400	4.5	3
600	7	5

In general, for any property, x , its average $\langle x \rangle$ can be obtained from the probability distribution $\varphi^N(l)$ in the following way: if we consider an ensemble of Z molecules, each with N double bonds, then

$$\begin{aligned} \langle x \rangle &= \frac{1}{Z} \sum_{\text{all seg, all mol}} x = \frac{1}{Z} \sum_l N(l)x(l) \\ &= \frac{1}{Z} \sum_l N_{\text{tot,seg}} \varphi^N(l)x(l), \end{aligned} \quad (7)$$

where $\varphi^N(l) = N(l)/N_{\text{tot,seg}}$, with $N(l)$ the number of segments with length l in the ensemble and $N_{\text{tot,seg}}$ the total number of segments. Finally,

$$\frac{\langle x \rangle}{N} = \left\langle \frac{1}{l} \right\rangle \sum_l \varphi^N(l)x(l), \quad (8)$$

where $\langle (1/l) \rangle$ is $1/N$ times the average number of segments per molecule or $\sum_l [\varphi^N(l)/l]$.

We now proceed to calculate $\varphi^N(l)$. Consider an open chain with N double bonds and k breaks, or “flips” as defined above, in the $N-1$ single bonds so that $k+1$ segments constitute the chain. The i th segment has length n_i . The probability of having a segment of length l in this molecule, $P_k^N(l)$, is given by

$$\begin{aligned} P_k^N(l) &= M_k^N \sum_{n_1=1}^N \sum_{n_2=1}^N \cdots \sum_{n_{k+1}=1}^N \delta \left(N - \sum_{i=1}^{k+1} n_i \right) \\ &\quad \times [\delta(n_1 - l) + \cdots + \delta(n_{k+1} - l)] \end{aligned}$$

with normalization factor M_k^N . Recognizing that all terms are equivalent, and using the exponential form of the delta function we obtain

$$\begin{aligned} P_k^N(l) &= M_k^N (k+1) \sum_{n_2} \cdots \sum_{n_{k+1}} \int_0^{2\pi} \exp \left[i\theta \left(N - l - \sum_{i=2}^{k+1} n_i \right) \right] \\ &\quad \times \frac{d\theta}{(2\pi)}. \end{aligned}$$

After performing the summations and some algebra,

$$P_k^N(l) = M_k^N (k+1) \frac{(N-1-l)!}{(N-k-l)!}.$$

To obtain the normalization factor from $\sum_{l=1}^{N-k} P_k^N(l) = 1$, we redefine $M_k^N = M_k^N (k+1)$, and use $\sum_{l=1}^{N-k} [(N-l-1)! / (N-k-l)!] = [(N-1)! / k(N-k-1)!]$. Finally,

$$P_k^N(l) = \frac{k(N-k-1)!(N-l-1)!}{(N-1)!(N-k-l)!} \quad \text{for } k \neq 0$$

and

$$P_0^N(l) = \delta_{N,l}.$$

The total probability of having a segment of length l , is $P_k^N(l)$ multiplied by the probability of k breaks in a length of N double bonds, which is given by $C_k^{N-1} p^{N-1-k} q^k$ (C_k^{N-1} being the same binomial coefficient as previously). Therefore,

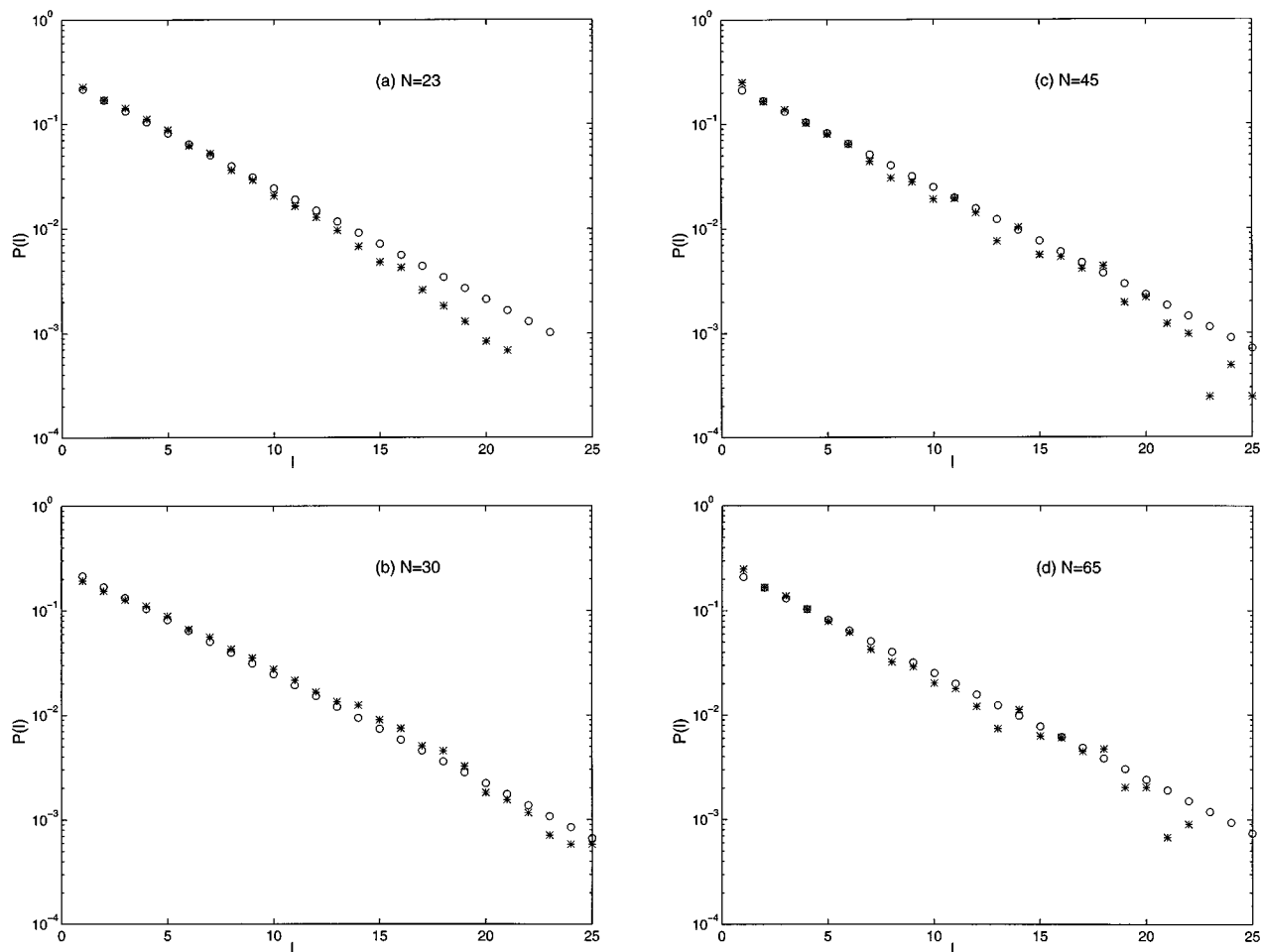


FIG. 3. Probability distribution of a segment of l double bonds in chains of (a) $N=23$; (b) $N=30$; (c) $N=45$; (d) $N=65$ double bonds from theory (O) and simulation (*).

$$\varphi^N(l) = \sum_{k=1}^{N-l} p^{N-1-k} q^k \frac{(N-1-l)!}{(N-l-k)!} \frac{k(N-1-k)!(N-1)!}{(N-1)!(N-1-k)!k!}. \quad (9)$$

p here corresponds to having two consecutive coplanar platelets, and, similarly, $q=1-p$ to having a flip or break in conjugation.

Simplifying the equation and renaming $\kappa=k-1$, we obtain

$$\begin{aligned} \varphi^N(l) &= p^{N-2} q \sum_{k=0}^{N-l-1} \left(\frac{q}{p}\right)^k C_k^{N-l-1} \\ &= p^{N-2} q \left(1 + \frac{q}{p}\right)^{N-l-1} \\ &= \frac{p^{N-2} q}{p^{N-l-1} (p+q)^{N-l-1}}, \quad \varphi^N(l) = p^{l-1} q. \end{aligned} \quad (10)$$

Since p is the probability of having two single bonds coplanar, it can be related to the number of flips in the chain in the following way:

$$p = \frac{N-1-m^*}{N-1},$$

where m^* is the most probable number of flips in a chain of $N-1$ single bonds. If the large N limit is assumed, m^* is given by Eq. (6), so that

$$p = \frac{N-1 - N e^{-(E_s+E_c)/kT}}{N-1}. \quad (11)$$

Comparison with simulations (Sec. IV) is good as can be seen in Fig. 3. As expected, there is better agreement with increasing N .

IV. SIMULATIONS

In addition to the analytical model described above, the effect of conformational disorder on conjugated systems and their optical properties was also studied through numerical simulations. To test the validity of the fragmentary chain picture we used the full Hamiltonian of Eq. (1). We find that the results of those simulations agree with the predictions of our analytical model. A Metropolis algorithm¹⁴ was employed—instead of choosing configurations randomly and then weighing them with a Boltzmann weight, we choose them with a probability $e^{-\beta H}$ and then weigh them equally. Configurations are produced by randomly moving one angle at a time in succession along the chain. The total energy is

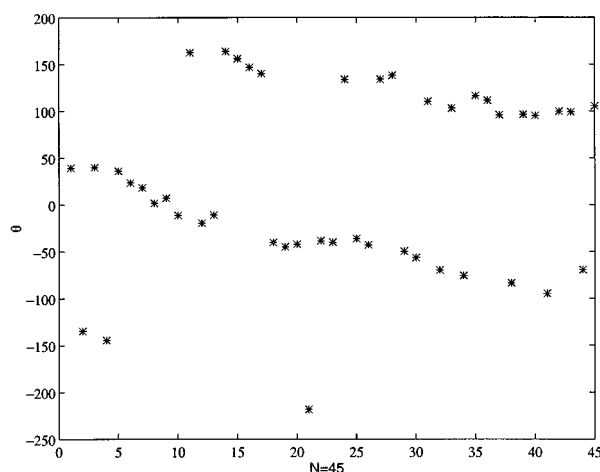


FIG. 4. Typical configuration of a chain of 45 double bonds from the simulations.

calculated by diagonalizing the Hamiltonian of Eq. (1) for that configuration. The average of any property, y , is then

$$\langle y \rangle = 1/M \sum_{i=1}^M y_i, \quad (12)$$

where y_i is the value of the property y of the i th configuration. M is the total number of configurations. Typically, M is 5000N in our case. The first configuration is randomly generated and configurations contribute to averages only after “equilibrium” is reached. From the equilibrium configurations, we extract information about the chain distortion. For the cases we considered, the notion of the fragmentary chain is appropriate. First, we observe that the overwhelming majority of angles is indeed close to zero as discussed in the previous section. We found flips as defined in Sec. III and almost planar segments between flips. A typical configuration for $N=45$ can be seen in Fig. 4. Note the appearance of flips. We performed the simulations at three different temperatures, $T=300, 400, 600$ K; for five different ratios of transfer integrals t_s/t_d from 0.3 to 0.8; for values of the steric energy parameter V_0 between 0.026 and 0.0033 eV; and for chains between 30 and 130 C atoms.

We also calculated the linear polarizability α . For each configuration, we use the standard expression from perturbation theory

$$\alpha = 2 \sum_n' \frac{\langle G|\mu|n \rangle \langle n|\mu|G \rangle}{E_n - E_G}, \quad (13)$$

where $\langle G|\mu|n \rangle$ is the transition moment matrix element between an excited and the ground state, and we obtain the average according to Eq. (12). All matrix elements are computed within the tight-binding approximation. With a centrosymmetric position system and within the one electron approximation, $\langle G|\mu|n \rangle$ becomes $\sum_i c_i^{\dagger ho} c_i^{el} z_i$, where z_i is the distance of site i from the origin—the center of the chain in our case—and $c_i^{\dagger ho} c_i^{el}$ the eigenfunctions of the hole and the electron, respectively, of the excited state $|n \rangle$. The original choice for V_0 , t_s , and t_d , as commented in Sec. II, is

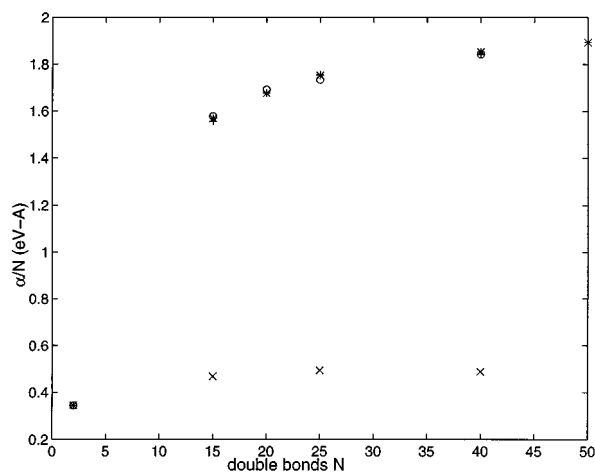


FIG. 5. α/N from simulations. (+) $V_0=0.026$ eV, $t_s=2.15$ eV, $t_d=2.85$ eV. (*) $V_0=0.013$ eV, $t_s=2.15$ eV, $t_d=2.85$ eV. (○) $V_0=0.0065$ eV, $t_s=2.15$ eV, $t_d=2.85$ eV. (×) $V_0=0.026$ eV, $t_s=1.52$ eV, $t_d=2.85$ eV.

0.026, 2.15, and 2.85 eV, respectively. Note from Fig. 5 the striking dependence of the linear polarizability to the transfer integrals ratio, and the insensitivity to the steric parameter. This is fortunate since the transfer integrals can be computed from experimental measurements of the band gap and bandwidth, while the steric parameter determination is based on cruder methods. The dependence on the ratio of transfer integrals is evident in our calculations of Sec. III.

V. OPTICAL PROPERTIES: α , γ , AND ABSORPTION

With an analytical expression for the probability of occurrence of a planar segment of length l in a chain of N double bonds, we can calculate any physical property of the system and compare with numerical simulations and experiments to test the relevance and applicability of the proposed picture of the chain as a collection of small planar segments. Extensive discussion of the optical properties can be found elsewhere.¹⁵ Here we will comment only briefly on optical properties, since they will be discussed in a forthcoming paper. We will show that there is agreement with numerical experiments, and that we are able to explain many of the features of recent experiments on long chains.⁹

We calculate these properties according to our proposed model of Eq. (8), as was explained in Sec. III. Here, $x(l)$ is the value of the property of a completely planar all trans chain with $2l$ carbon atoms. For $\alpha(l)$, we use the expression of Eq. (13). For $\gamma(l)$, we follow the approach of Yaron *et al.*¹²

We compare with the simulations in the following way: we use the configurations generated by the simulations, after diagonalization of the electronic and steric Hamiltonian of Eq. (1), and calculate α in the manner explained in Sec. IV and γ according to Ref. 12. We compare with the predictions of our analytical model, which uses the probability distribution of Eqs. (10)–(11). The values of the parameters are again, $V_0=0.026$ eV, $t_s=2.15$ eV, and $t_d=2.85$ eV. The agreement can be seen in Figs. 6 and 7. Our analytical model

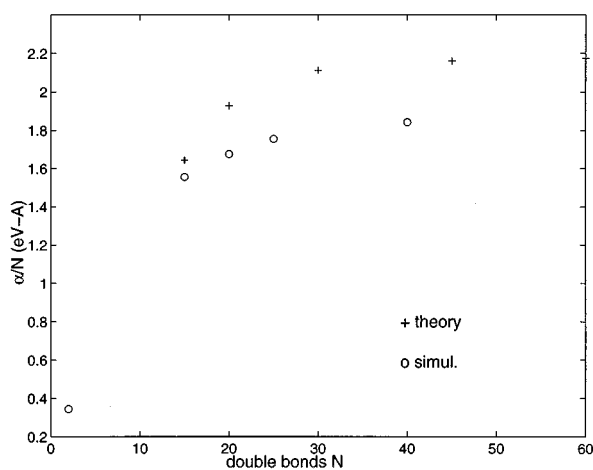


FIG. 6. α/N from simulations and theory, $V_0=0.026$ eV, $t_s=2.15$ eV, $t_d=2.85$ eV.

captures the behavior of the system. When we compare our results with that of recent experiment,⁹ we can immediately see that our saturation value for γ/N is close to the experimental value [14.5×10^{-34} vs 16×10^{-34} electrostatic units (esu), respectively]. In our model, the saturation is reached for chains of ≈ 80 carbons (40 double bonds), longer than theoretically predicted for the fully planar all trans molecule (≈ 20 – 30 double bonds),^{12,16,17} and shorter than seen in the experiment (saturation at 240 carbons). This latter discrepancy may be partly due to the phenyl ring in the middle of the molecules used in the experiment, which may cause the chains to behave as half the length originally thought, as noted already by Samuel *et al.*⁹ Also, note that there is an uncertainty in the value of the steric potential constant, V_0 , used. We have used a value for V_0 which may need to be modified for the particular molecules of the experiment.

We also study the absorption of long chains. We model the absorption of the $1^1A_g \rightarrow 1^1B_u$ electronic transition of a polyene of length l , by

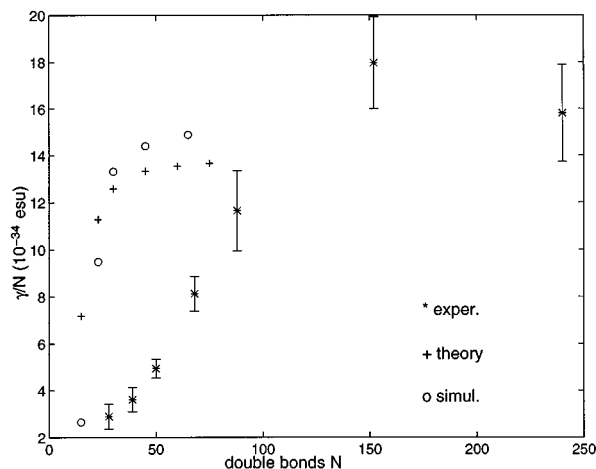


FIG. 7. γ/N from simulations, theory, and experiment.

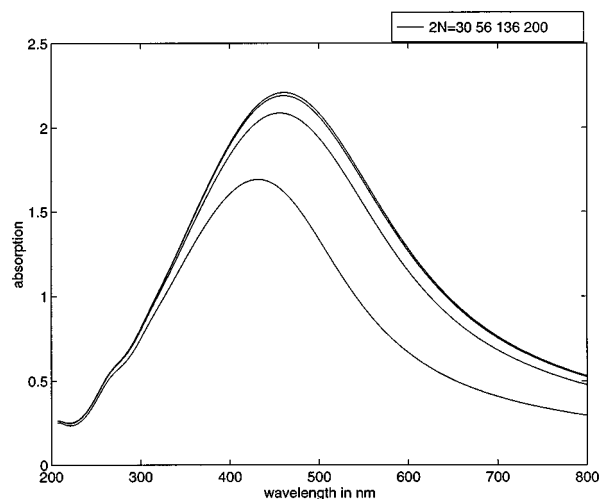


FIG. 8. Absorption spectrum from theory.

$$I_l(\omega) = \frac{\delta/\pi}{(\omega - \omega_l)^2 + \delta^2} \mu_l^2,$$

where $\omega_l = A + B/l$ can be obtained by fitting experimental data in the usual way, and μ is obtained in the same manner as described in Sec. IV. So the absorption of a chain of N double bonds is given, according to our model by Eq. (8),

$$\langle I(\omega) \rangle = \sum_l \frac{\delta/\pi}{(\omega - \omega_l)^2 + \delta^2} \mu_{ell}^2 \phi^N(l).$$

As in the case with γ , we observe a faster “saturation” than the experiment (Fig. 8).

VI. CONCLUSION

Starting from a microscopic description, we propose an alternative way to consider conformational disorder on conjugated chains. Instead of focusing on the majority of small angular deviations of adjacent platelets, we consider the few big breaks or “flips.” We propose that the distribution of the length of the segments between flips is the most relevant for the optical properties of these chains. Our predictions are supported by numerical simulations. Certain aspects of recent experimental observations are also accounted for. In the process, we derive the form of the phenomenological term used to describe the conjugation effect of these systems and relate its parameters to measurable quantities, but retain the phenomenological form of the steric interactions. Further work on this is in progress.

ACKNOWLEDGMENT

This work was supported primarily by the MRSEC program of the NSF under award number DMR 9400334.

¹R. H. Baughman and R. R. Chance, *J. Chem. Phys.* **47**, 4295 (1976).

²G. Rossi, R. R. Chance, and R. J. Silbey, *J. Chem. Phys.* **90**, 7594 (1989).

³G. Rossi and A. Viallat, *Phys. Rev. B* **40**, 10 036 (1989); *J. Chem. Phys.* **92**, 4548 (1990); A. Viallat, *ibid.* **92**, 4557 (1990).

- ⁴P. A. Pincus, G. Rossi, and M. E. Gates, *Europhys. Lett.* **4**, 41 (1987).
- ⁵R. MacKenzie, J. M. Ginger, and A. J. Epstein, *Phys. Rev. B* **44**, 2362 (1991).
- ⁶J. L. Brédas, C. Quattrochi, J. Libent, A. C. MacDiarmid, J. M. Ginger, and A. J. Epstein, *Phys. Rev. B* **44**, 6002 (1991).
- ⁷Z. G. Soos and K. S. Schweizer, *Chem. Phys. Lett.* **139**, 196 (1987).
- ⁸B. E. Kohler and I. D. W. Samuel, *J. Chem. Phys.* **103**, 6248 (1995); B. E. Kohler and J. C. Woehl, *J. Chem. Phys.* **103**, 6253 (1995).
- ⁹I. D. W. Samuel, I. Ledoux, C. Dhenaut, J. Zyss, H. H. Fox, R. R. Schrock, and R. J. Silbey, *Science* **265**, 1070 (1994).
- ¹⁰K. S. Scheizer, *J. Chem. Phys.* **85**, 4181 (1985); **85**, 1156, 1176 (1986). (1986).
- ¹¹W. P. Su, J. R. Schrieffer, and A. S. Heeger, *Phys. Rev. B* **22**, 2099 (1980).
- ¹²D. Yaron and R. J. Silbey, *Phys. Rev. B* **45**, 11 655 (1992).
- ¹³J. R. Ackerman and B. E. Kohler, *J. Chem. Phys.* **80**, 45 (1984).
- ¹⁴N. Metropolis, A. W. Ronenbluth, M. N. Rosenbluth, A. H. Teller, and E. Teller, *J. Chem. Phys.* **21**, 1087 (1953).
- ¹⁵I. D. W. Samuel *et al.* (unpublished).
- ¹⁶S. Mukamel, A. Takahashi, H. X. Wang, and G. H. Chen, *Science* **266**, 250 (1994).
- ¹⁷F. C. Spano and Z. G. Soos, *J. Chem. Phys.* **99**, 9265 (1993).